

# Emergent $p$ -wave Kondo Coupling in Multi-Orbital Bands with Mirror Symmetry Breaking

Jun Won Rhim<sup>1,\*</sup> and Jung Hoon Han<sup>2,3</sup>

<sup>1</sup>*School of Physics, Korea Institute for Advanced Study, Seoul 130-722, Korea*

<sup>2</sup>*Department of Physics and BK21 Physics Research Division, Sungkyunkwan University, Suwon 440-746, Korea*

<sup>3</sup>*Asia Pacific Center for Theoretical Physics, Pohang, Gyeongbuk 790-784, Korea*

(Dated: August 12, 2021)

We examine Kondo effect in the periodic Anderson model for which the conduction band is of multi-orbital character and subject to mirror symmetry breaking field imposed externally. Taking  $p$ -orbital-based toy model for analysis, we find the Kondo pairing symmetry of  $p$ -wave character emerges self-consistently over some regions of parameter space and filling factor even though only the on-site Kondo hybridization is assumed in the microscopic Hamiltonian. The band structure in the Kondo-hybridized phase becomes nematic, with only two-fold symmetry, due to the  $p$ -wave Kondo coupling. The reduced symmetry should be readily observable in spectroscopic or transport measurements for heavy fermion system in a multilayer environment such as successfully grown recently.

PACS numbers: 71.27.+a, 73.20.-r, 75.30.Mb

*Introduction.*- State-of-the-art technique to grow heavy fermion compounds with atomic thickness precision has been achieved in recent years [1, 2]. Heavy fermion phase and superconductivity were identified in CeCoIn<sub>5</sub> layer of less than one nanometer thickness grown in this manner, prompting speculations of exotic new phases in atomically thin heterostructure [2]. Apart from the novelty of reduced dimensionality, the alternate stacking of heavy fermion layer with normal metal YbCoIn<sub>5</sub> layer realized in the growth process is likely to give rise to new physical phenomena by virtue of the mirror symmetry breaking (MSB) at the interface. Aspects of non-centrosymmetric superconductivity have been exhaustively studied since its original discovery in the heavy-fermion compound CePt<sub>3</sub>Si [3]. The heavy fermion multilayer structure, on the other hand, differs from the conventional non-centrosymmetric material in that the violation of symmetry is macroscopically imposed (not microscopically at the level of crystal structure) and, with recently available techniques such as electrolyte gating, controllable. Due to the thin layer thickness, such MSB is likely to infect the entire heavy fermion band structure and therefore the nature of emerging Kondo and/or superconducting pairing as well. Some consequences of the MSB in the heavy fermion multilayer have been studied theoretically by Maruyama *et al.* quite recently [4], where the main focus was on the novel superconducting pairing symmetries and other thermodynamic properties induced by the phenomenological Rashba term.

It has been customary in the past to regard the Rashba interaction as a relativistic effect manifesting itself in a mirror symmetry-broken environment. Several recent papers [5–7], however, have shown that multi-orbital degeneracy, in addition to MSB, is an essential pre-requisite for the manifestation of strong Rashba coupling in the

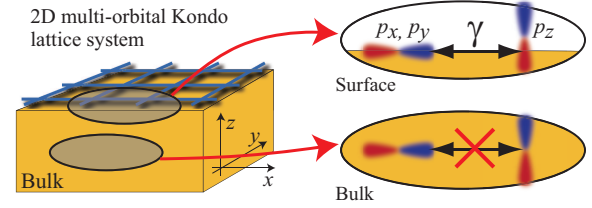


FIG. 1: (Color online) Schematic picture of Kondo lattice model subject to mirror symmetry breaking at the surface or interface. Hopping processes between, for instance,  $p_z$  and  $p_{x,y}$  otherwise forbidden in the bulk become possible due to the symmetry breaking field as shown in the upper right cartoon.

electron dynamics. In this new picture Rashba interaction becomes an electrostatic effect with its magnitude dictated by the degree of orbital asymmetry about the mirror plane (see Fig. 1) [5–7].

In fact Kondo lattice behavior takes place in an orbital-rich environment with the extended  $p$ - or  $d$ -orbital states forming the conduction bands while the localized moments arise from  $f$ -orbitals [8, 9]. Using our recent experience with the Rashba phenomena in non-Kondo materials as a guide, we present a faithful modeling of Kondo lattice behavior where multi-orbital degrees of freedom in a mirror symmetry-broken environment are explicitly embedded in the conduction band Hamiltonian. The use of Rashba interaction as a purely phenomenological addition, as is often done in the current literature, is avoided. Our approach differs as well from the large- $N$  generalization of the one-band Kondo lattice model, where  $N$  identical copies with the same orbital symmetry are adopted as a way to justify

the mean-field approximation [9]. In reality the MSB field - usually the electric field acting perpendicular to the interface or the surface - influences orbitals which are extended along the field direction more than those which extend in the orthogonal direction. Conventional one-band or large- $N$  approach assuming featureless orbitals will not capture this effect properly.

*The model.*- Choosing the degenerate  $p$ -orbital states hopping on a square lattice as a toy example, we write down the Hamiltonian [6, 7]

$$H_{\text{MSB}} = \sum_{\mathbf{k}\lambda\sigma} \left( \epsilon_{\mathbf{k}}^{\lambda} p_{\lambda\mathbf{k}\sigma}^{\dagger} p_{\lambda\mathbf{k}\sigma} + 3\gamma i s_{\lambda} p_{z\mathbf{k}\sigma}^{\dagger} p_{\lambda\mathbf{k}\sigma} + \text{h.c.} \right) + \sum_{\mathbf{k}\sigma} \mu_f f_{\mathbf{k}\sigma}^{\dagger} f_{\mathbf{k}\sigma} \quad (1)$$

for the dispersive  $p$ -orbital ( $p_{\lambda\mathbf{k}\sigma}$ ) bands and a single pair of localized Kramers doublet ( $f_{\mathbf{k}\sigma}$ ) with on-site energy  $\mu_f$ . The orbital index  $\lambda \in \{x, y, z\}$  spans the three  $p$ -orbital states of the conduction band and  $\sigma = +(-)$  is the spin up(down). One can show, employing the two Slater-Koster parameters  $V_1, V_2$  for  $\sigma$ - and  $\pi$ -bonding of  $p$ -orbitals, that  $\epsilon_{\mathbf{k}}^{\lambda} = -2(V_1 + V_2)c_{\lambda} + 2V_2(c_x + c_y)$  with  $c_x(y) = \cos k_{x(y)}, s_x(y) = \sin k_{x(y)}$  and  $c_z = s_z = 0$  for the assumed two-dimensional bands. Mirror symmetry breaking is reflected in the second term of Eq. (1), proportional to the MSB parameter  $\gamma$  [7]. They give the hybridization of  $p_z$ -orbital with  $p_x$ - and  $p_y$ -orbitals; these are processes normally forbidden by symmetry if a mirror plane existed. This kind of symmetry breaking is realized naturally on the surface of a bulk material or by applying vertical electric field to the planar system as illustrated in Fig. 1.

Secondly the Kondo hybridization of local and itinerant spins follows from the Heisenberg-type exchange interaction  $H_K = J_K \sum_{i,\lambda} \mathbf{S}_{i\lambda} \cdot \mathbf{S}_{if}$ , with spin-1/2 operators made out of  $p_{\lambda}$ -orbital ( $\mathbf{S}_{i\lambda}$ ) and  $f$ -orbital ( $\mathbf{S}_{if}$ ), respectively. Finally  $H_{\text{SOC}} = (\alpha/2) \sum_i \mathbf{L}_i \cdot \boldsymbol{\sigma}_i$  involving the  $p$ -orbital angular momentum operator ( $L = 1$ )  $\mathbf{L}_i$  and the spin-1/2 operator  $(1/2)\boldsymbol{\sigma}_i$  at each site  $i$  gives the spin-orbit coupling (SOC) within the  $p$ -orbital bands. In typical heavy fermion matter such as CeCoIn<sub>5</sub> the heavy element In playing a main role in the conduction band structure will also carry substantial amount of spin-orbit energy  $\alpha$ .

The total Hamiltonian  $H = H_{\text{MSB}} + H_{\text{SOC}} + H_K$  can be handled within the framework of renormalized mean-field theory [10–12] which decomposes the Kondo exchange interaction as ( $\bar{\sigma} = -\sigma$ )

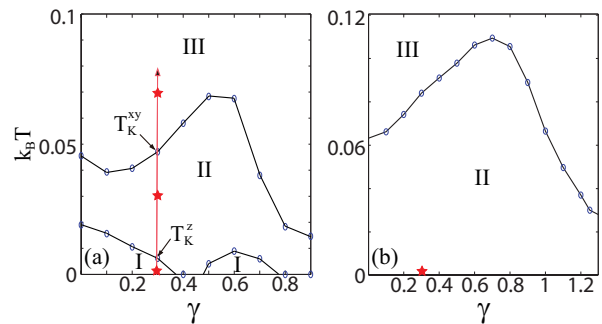


FIG. 2: (Color online) Phase diagrams with (a)  $\alpha = 0$  (no SOC),  $n_c = 2$  and (b)  $\alpha = 0.5$  (SOC),  $n_c = 1.5$ . Phase I denotes all three  $p$ -orbitals hybridized ( $h_{\sigma}^x, h_{\sigma}^y, h_{\sigma}^z \neq 0$ ). Phase II represents only  $p_x, p_y$  orbitals hybridized ( $h_{\sigma}^x \neq 0, h_{\sigma}^y \neq 0, h_{\sigma}^z = 0$ ). Phase III is trivial with no Kondo hybridization ( $h_{\sigma}^z = 0$ ). In (a), as shown by a red vertical arrow, we may encounter two distinct Kondo temperatures labeled by  $T_K^{xy}$  and  $T_K^z$ . Parameters used to obtain both phase diagrams are  $(V_1, V_2, J_K) = (2, 0.65, 3)$ . Fermi surface structures at the four points indicated by stars are shown in Fig. 3.

$$H_K = \frac{J_K}{2} \sum_{i\lambda\sigma} \left( \frac{b_{\bar{\sigma}\sigma}^{\lambda}}{2} p_{\lambda i\bar{\sigma}}^{\dagger} f_{i\bar{\sigma}} - h_{\sigma}^{\lambda} p_{\lambda i\sigma}^{\dagger} f_{i\sigma} + \text{h.c.} \right) + \frac{J_K}{2} \sum_{i\sigma} \Gamma_{\sigma}^p f_{i\bar{\sigma}}^{\dagger} f_{i\sigma} + \frac{J_K}{2} \sum_{i\lambda\sigma} \Gamma_{\sigma}^f p_{\lambda i\bar{\sigma}}^{\dagger} p_{\lambda i\sigma}. \quad (2)$$

In addition to the Kondo hybridization parameters  $b_{\sigma\sigma'}^{\lambda} = \langle f_{i\sigma}^{\dagger} p_{\lambda i\sigma'} \rangle$  and  $h_{\sigma}^{\lambda} = b_{\sigma\sigma}^{\lambda} + b_{\bar{\sigma}\bar{\sigma}}^{\lambda}/2$ , we also allow same-orbital spin-flip processes encoded by  $\Gamma_{\sigma}^p = \sum_{\lambda} \langle p_{\lambda i\sigma}^{\dagger} p_{\lambda i\bar{\sigma}} \rangle$  and  $\Gamma_{\sigma}^f = \langle f_{i\bar{\sigma}}^{\dagger} f_{i\sigma} \rangle$ . The spin-flip parameters  $\Gamma_{\sigma}^p, \Gamma_{\sigma}^f$ , and  $b_{\bar{\sigma}\bar{\sigma}}^{\lambda}$  can be nonzero due to the spin-orbit interaction. We restrict ourselves however to non-magnetic, singlet Kondo coupling in the mean-field scheme and avoid the possibility of Kondo pairing between remote sites [10], which is another known avenue to obtain non- $s$ -wave Kondo pairing. The fact that our model can exhibit the  $p$ -wave Kondo phase despite the on-site-only Kondo hybridization Hamiltonian  $H_K$  emphasizes the emergent nature of unconventional pairing. As demonstrated in Refs. [5–7], Rashba interaction is another emergent property of the band that can be derived from the underlying microscopic Hamiltonian consisting only of  $H_{\text{MSB}}$  and  $H_{\text{SOC}}$ .

*Phase diagram.*- All the hybridization parameters can be determined self-consistently, along with  $\mu_f$  to ensure  $(\sum_{\sigma} f_{i\sigma}^{\dagger} f_{i\sigma}) = 1$ , and the overall chemical potential  $\mu$ , for various input band structure parameters  $V_1, V_2, \gamma$ , electron filling factor  $n_c = (\sum_{\lambda\sigma} p_{\lambda i\sigma}^{\dagger} p_{\lambda i\sigma})$ , at various temperatures  $T$ . Generic phase diagrams resulting from our model Hamiltonian are plotted in Fig. 2 in the space of temperature  $T$  and MSB parameter  $\gamma$  with and without the SOC. We observe two distinct Kondo-coupled

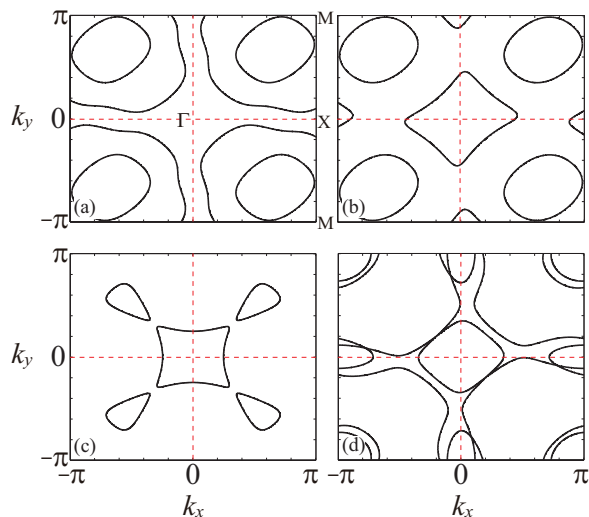


FIG. 3: (Color online) Band dispersions at the Fermi level for the various phases marked by red stars ( $\star$ ) in Fig. 2. (a), (b) and (c) are the Fermi surfaces of the phases I, II and III in Fig. 2(a) respectively, and (d) corresponds to the star in Fig. 2(b). The reduced symmetry in the Kondo-coupled phases (a), (b), and (d) due to the  $p$ -wave Kondo pairing are apparent against the  $(k_x, k_y)$  axes in red dashed lines.

phases labeled I in Fig. 2, where all three  $p$ -orbitals hybridize with  $f$ -orbital ( $h_\sigma^x, h_\sigma^y, h_\sigma^z \neq 0$ ), and II where only the in-plane  $p_x, p_y$  orbitals hybridize ( $h_\sigma^z = 0$ ). The high-temperature non-Kondo phase with  $h_\sigma^\lambda = 0$  is labeled III. Both transitions, I $\rightarrow$ II and II $\rightarrow$ III, are second-order. Phase I becomes unstable and gives way to phase II as shown in Fig. 2(b) as the strength of SOC is increased. Although the addition of SOC complicates the microscopic Hamiltonian, fortunately, many of the hybridization parameters were found to be vanishing  $\Gamma_\sigma^p = \Gamma_\sigma^f = b_{\sigma\sigma}^z = b_{\sigma\bar{\sigma}}^x = b_{\sigma\bar{\sigma}}^y = 0$  even with finite SOC. Features of the phase diagram are dependent on the filling factor  $n_c$  of  $p$ -electrons. Phase I is observed within a small range of  $n_c$  and, as indicated in Fig. 2(a), may even exhibit some re-entrant behavior with increasing  $\gamma$ . While the details regarding the extent of each Kondo phase or the Kondo temperature are sensitive to the occupation  $n_c$ , the effect of SOC on them was found to be much less significant by comparison.

*Effective Hamiltonian for  $p$ -wave Kondo pairing.*— Most interestingly, the two Kondo-coupled phases I and II exhibit the band dispersion with the loss of symmetry under the reflection  $(k_x, k_y) \rightarrow (-k_x, k_y)$  or  $(k_x, k_y) \rightarrow (k_x, -k_y)$ , as well as the  $90^\circ$  rotation, as shown in Fig. 3. Reduction in the band structure symmetry only occurs in the Kondo phase implying that it can only be the consequence of  $p$ -wave Kondo coupling. Below we show rigorously how such unconventional pairing occurs for MSB-infected bands.

With a proper choice of tight binding parameters and filling factors we can identify cases in the self-consistent band structure wherein the two lowest-energy spin-orbit coupled  $p$ -orbital bands and the two Kramers doublet  $f$ -electron bands occur in the vicinity of the Fermi energy while all others are further removed from it. In such cases one can describe the Kondo physics within the projected Hilbert space of those four bands associated with the following operators:

$$\tilde{c}_{n\mathbf{k}} = \sum_{\lambda\sigma} v_{\lambda\mathbf{k}\sigma}^n p_{\lambda\mathbf{k}\sigma} \quad \text{and} \quad \tilde{f}_{\mathbf{k}\sigma} = f_{\mathbf{k}\sigma} + \sum_{n=3}^6 u_{\mathbf{k}\sigma}^n \tilde{c}_{n\mathbf{k}}. \quad (3)$$

Here,  $n = 1 - 6$  labels the six  $p$ -orbital bands of  $H_{\text{MSB}} + H_{\text{SOC}}$ , the state at  $\mathbf{k}$  being denoted  $|\mathbf{v}_{\mathbf{k}}^n\rangle = \tilde{c}_{n\mathbf{k}}^\dagger |0\rangle$  with the coefficients  $v_{\lambda\mathbf{k}\sigma}^n$ . The localized  $f$ -electron operator is modified through Kondo hybridization with the higher energy bands,  $u_{\mathbf{k}\sigma}^n = \langle \mathbf{v}_{\mathbf{k}}^n | H_{\text{K}} | f_{\mathbf{k}\sigma} \rangle / (\mu_f - \varepsilon_{n\mathbf{k}}^c)$ ,  $n = 3 - 6$ , where  $\varepsilon_{n\mathbf{k}}^c$  is the energy of  $n$ -th band of  $H_{\text{MSB}} + H_{\text{SOC}}$  and  $|f_{\mathbf{k}\sigma}\rangle = f_{\mathbf{k}\sigma}^\dagger |0\rangle$ . The effective Hamiltonian within the reduced Hilbert space of  $\{|\mathbf{v}_{\mathbf{k}}^1\rangle, |\mathbf{v}_{\mathbf{k}}^2\rangle, |\tilde{f}_{\mathbf{k}+}\rangle, |\tilde{f}_{\mathbf{k}-}\rangle\}$ , where  $|\tilde{f}_{\mathbf{k}\sigma}\rangle = \tilde{f}_{\mathbf{k}\sigma}^\dagger |0\rangle$ , is

$$H_{\text{eff}} = \sum_{n=1,2} \varepsilon_{n\mathbf{k}}^c \tilde{c}_{n\mathbf{k}}^\dagger \tilde{c}_{n\mathbf{k}} + \sum_{\sigma} \varepsilon_{\sigma\mathbf{k}}^f \tilde{f}_{\mathbf{k}\sigma}^\dagger \tilde{f}_{\mathbf{k}\sigma} + \sum_{n=1,2,\sigma} \left( V_{\mathbf{k}}^{n\sigma} \tilde{c}_{n\mathbf{k}}^\dagger \tilde{f}_{\mathbf{k}\sigma} + \text{h.c.} \right). \quad (4)$$

The  $f$ -level dispersion  $\varepsilon_{\sigma\mathbf{k}}^f$  and the effective Kondo coupling  $V_{\mathbf{k}}^{n\sigma} = \langle \mathbf{v}_{\mathbf{k}}^n | H_{\text{K}} | f_{\mathbf{k}\sigma} \rangle$  are given by

$$\varepsilon_{\sigma\mathbf{k}}^f = \mu_f + \sum_{n=3}^6 \frac{|\langle \mathbf{v}_{\mathbf{k}}^n | H_{\text{K}} | f_{\mathbf{k}\sigma} \rangle|^2}{\mu_f - \varepsilon_{n\mathbf{k}}^c},$$

$$V_{\mathbf{k}}^{n\sigma} = \frac{J_{\text{K}}}{2} \left( \frac{1}{2} b_{\sigma\bar{\sigma}}^z v_{z\mathbf{k}\bar{\sigma}}^n - h_{\sigma\bar{\sigma}}^x v_{x\mathbf{k}\sigma}^n - h_{\sigma\bar{\sigma}}^y v_{y\mathbf{k}\sigma}^n \right). \quad (5)$$

Some properties of the self-consistently obtained hybridization parameters of Kondo-coupled phases such as  $\Gamma_\sigma^p = \Gamma_\sigma^f = b_{\sigma\sigma}^z = b_{\sigma\bar{\sigma}}^x = b_{\sigma\bar{\sigma}}^y = 0$  are used to derive the above effective Hamiltonian. The energy dispersion obtained from  $H_{\text{eff}}$  matches the full dispersion almost exactly. Characteristics of the Kondo-coupled bands can be discussed faithfully now in terms of the effective Hamiltonian,  $H_{\text{eff}}$ .

The effective Kondo coupling  $V_{\mathbf{k}}^{n\sigma}$  appearing in  $H_{\text{eff}}$  has the explicit momentum dependence despite the fact that the original Hamiltonian only contained the on-site Kondo interaction. The symmetry of the Kondo pairing, self-consistently determined to be  $p$ -wave as illustrated in Fig. 4, also dictates that of the hybridized bands, as shown in Fig. 3. The symmetry properties of  $V_{\mathbf{k}}^{n\sigma}$ , in turn, follow from those of the wave functions  $v_{\lambda\mathbf{k}\sigma}^n$  as outlined in Table I.

$\mathbf{k}$	wave function
$(k_x, k_y)$	$\{v_{x\mathbf{k}+}^n, v_{y\mathbf{k}+}^n, v_{z\mathbf{k}+}^n, v_{x\mathbf{k}-}^n, v_{y\mathbf{k}-}^n, v_{z\mathbf{k}-}^n\}$
$(-k_x, k_y)$	$\{-v_{x\mathbf{k}+}^{n*}, v_{y\mathbf{k}+}^{n*}, -v_{z\mathbf{k}+}^{n*}, -v_{x\mathbf{k}-}^{n*}, v_{y\mathbf{k}-}^{n*}, -v_{z\mathbf{k}-}^{n*}\}$
$(k_x, -k_y)$	$\{v_{x\mathbf{k}+}^{n*}, -v_{y\mathbf{k}+}^{n*}, -v_{z\mathbf{k}+}^{n*}, -v_{x\mathbf{k}-}^{n*}, v_{y\mathbf{k}-}^{n*}, v_{z\mathbf{k}-}^{n*}\}$
$(-k_x, -k_y)$	$\{-v_{x\mathbf{k}+}^n, -v_{y\mathbf{k}+}^n, v_{z\mathbf{k}+}^n, v_{x\mathbf{k}-}^n, v_{y\mathbf{k}-}^n, -v_{z\mathbf{k}-}^n\}$
$(-k_y, k_x)$	$\{-v_{y\mathbf{k}+}^n, v_{x\mathbf{k}+}^n, v_{z\mathbf{k}+}^n, -iv_{y\mathbf{k}-}^n, iv_{x\mathbf{k}-}^n, iv_{z\mathbf{k}-}^n\}$

TABLE I: Relation between eigenstates of  $H_{\text{MSB}} + H_{\text{SOC}}$  at several symmetry-related momenta.  $v_{\lambda\mathbf{k}\sigma}^n$  in the first row refers to the amplitude of  $p_\lambda$ -orbital with spin  $\sigma$  for the eigenstate at  $\mathbf{k} = (k_x, k_y)$ ;  $\sigma = +(-)$  corresponds to spin up(down). Eigenstates at other momenta are related to this one as shown in the subsequent rows.

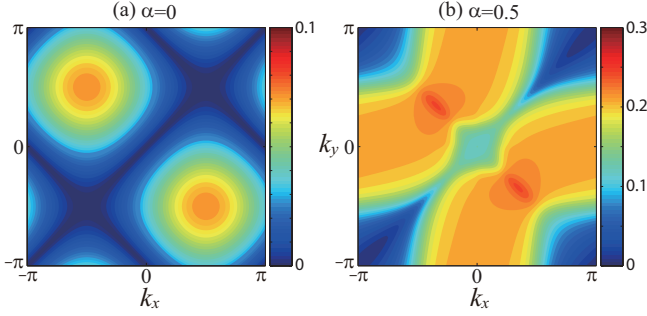


FIG. 4: (Color online) Contour plots of  $|V_{\mathbf{k}}^{1+}|$ , the absolute value of the effective Kondo hybridization, in the Brillouin zone. (a)  $\alpha = 0$  (no SOC) and (b)  $\alpha = 0.5$ .

Transformation rules for the wave functions are deduced by examining whether the Hamiltonians at a pair of symmetry-related momenta can transform into each other by some kind of unitary or anti-unitary operators such as  $K\sigma_z \otimes R_x(\pi)$ ,  $KI \otimes R_y(\pi)$ ,  $\sigma_z \otimes R_z(\pi)$  and  $e^{-i\frac{3}{4}\pi} D_z^{1/2}(3\pi/2) \otimes R_z(\pi/2)$ . We denote  $R_\lambda(\theta)$  for the SO(3) rotation matrix,  $\lambda = x, y, z$ ,  $D_z^{1/2}(\theta)$  for the SU(2) rotation matrix, and  $K$  for the complex conjugation. From the Table and Eq. (5) one can show that  $V_{-k_x, -k_y}^{n\sigma} = -\sigma V_{k_x, k_y}^{n\sigma}$ , and therefore a unitary transformation  $\sigma_z \otimes I$  between  $H_{\text{eff}}(\mathbf{k})$  and  $H_{\text{eff}}(-\mathbf{k})$  exists, ensuring the equivalence of the energies between  $\mathbf{k}$  and  $-\mathbf{k}$ . On the other hand  $V_{-k_x, k_y}^{n\sigma}$ ,  $V_{k_x, -k_y}^{n\sigma}$  and  $V_{-k_y, k_x}^{n\sigma}$  are not related to  $V_{k_x, k_y}^{n\sigma}$  in any way according to the Table I. For example,  $V_{-k_x, k_y}^{n\sigma} = J_K(-b_{\sigma\bar{\sigma}}^z v_{z\mathbf{k}\bar{\sigma}}^{n*}/2 + h_{\sigma}^x v_{x\mathbf{k}\sigma}^{n*} - h_{\sigma}^y v_{y\mathbf{k}\sigma}^{n*})/2$  does not even have the same magnitude as  $V_{\mathbf{k}}^{n\sigma}$  in general because the wave function  $v_{\lambda\mathbf{k}\sigma}^n$  are complex-valued. Referring to Eq. (5), neither the reflection about the  $x$ - or the  $y$ -axis nor the  $90^\circ$  rotation in  $\mathbf{k}$ -space is guaranteed to yield unitary-equivalent  $H_{\text{eff}}$ .

It is further possible to find an explicit expression of the effective Kondo coupling to prove its  $p$ -wave nature for models without SOC. Given the parameters such as  $V_1 = 2$ ,  $V_2 = 0.65$ ,  $\gamma = 0.3$  and the filling of conduction electrons  $n_c = 1.5$ , the band dispersions around

the M point meet the conditions assumed in deriving the effective Hamiltonian  $H_{\text{eff}}$ . Here one can show  $v_{\lambda\mathbf{k}\sigma}^n$  near  $\mathbf{k} = (\pi, \pi)$  is  $v_{x, y\mathbf{k}+}^1 \approx -3\gamma s_{x, y}/2(V_1 + V_2)$  and  $v_{x, y\mathbf{k}-}^1 = 0$ , and vice versa for  $n = 2$ . Turning off SOC, all spin-mixing mean field parameters  $b_{\sigma\bar{\sigma}}^z$  vanish. We can conclude only two equivalent ground states with real-valued Kondo parameters  $h_{\sigma}^x = h_{\sigma}^y$  or  $h_{\sigma}^x = -h_{\sigma}^y$  are possible, giving out

$$V_{\mathbf{k}} \equiv V_{\mathbf{k}}^{1+} = V_{\mathbf{k}}^{2-} = \frac{3iJ_K h^x \gamma}{4(V_1 + V_2)} (\sin k_x \pm \sin k_y) \quad (6)$$

and  $V_{\mathbf{k}}^{1-} = V_{\mathbf{k}}^{2+} = 0$  for  $h_{\sigma}^x = \pm h_{\sigma}^y$ , respectively. The effective Kondo coupling indeed has the  $p$ -wave symmetry with a node along the  $k_x = +k_y$  or  $k_x = -k_y$  line. Figure 4(b) shows the plot of  $|V_{\mathbf{k}}^{1+}|$  for the case of  $h_{\sigma}^x = -h_{\sigma}^y$  where the node extends along  $k_x = -k_y$ . It is also seen that  $p$ -wave Kondo coupling is not predicated on SOC at all.

Instead, the  $p$ -wave Kondo coupling is strictly a consequence of nonzero MSB,  $\gamma \neq 0$ . When  $\gamma = 0$ , Hamiltonian matrices of  $H_{\text{MSB}} + H_{\text{SOC}}$  at  $(k_x, k_y)$ ,  $(-k_x, k_y)$ ,  $(k_x, -k_y)$  and  $(-k_x, -k_y)$  are equal to each other [13]. As a result, those momenta have identical eigenvectors and, according to Eq. (5), the same Kondo coupling  $V_{\mathbf{k}}^{n\sigma}$ . In addition the  $p$ -wave character arises only when both  $h_{\sigma}^x$  and  $h_{\sigma}^y$  are nonzero. For phases I and II such condition is indeed achieved with  $|h_{\sigma}^x| = |h_{\sigma}^y|$ . The  $p$ -wave Kondo states are favored away from half-filling regime such as considered in the phase diagram of Fig. 2. At half filling  $n_c = 3$  without SOC, on the other hand, we often find the ground phase with only  $h_{\sigma}^z$  non-vanishing. In this case, the effective Kondo coupling is in the form  $V_{\mathbf{k}}^{n\sigma} = -J_K h_{\sigma}^z v_{z\mathbf{k}\sigma}^n/2 \approx iJ_K h_{\sigma}^z/2$ , which is  $s$ -wave as in the ordinary heavy fermion matter.

*Discussion.-* As the angstrom-scale deposition technique of thin films develops into maturity, the role of surface states with broken mirror symmetry takes on greater practical significance. Such MSB field effect leads to interesting consequences when acting on a multi-orbital environment such as the emergence of Rashba effect [6, 7], orbital-dependent spin transfer torque [14], and as argued in this work, of un-conventional Kondo pairing. Conventional one-band Kondo model with the phenomenological Rashba term could very well miss this feature due to the inadequate treatment of the multi-orbital character. The asymmetric band structure we found in the Kondo-coupled phase should be readily detected in the spectroscopic study such as ARPES, or in the transport measurements through their directional responses. Although proposals of non- $s$ -wave Kondo pairing are already available [10–12], they tend to trace its origin to the non-local character of Kondo coupling between localized and itinerant moments [10], or the orbital symmetry of the  $f$ -orbital localized moments [12]. By contrast,

the  $p$ -wave Kondo hybridization emerging in our scenario is a generic consequence of the macroscopic breaking of mirror symmetry imposed by the geometry of the heterostructure itself. Existing theory of heavy fermion heterostructure [4] focused on the nature of unconventional superconductivity resulting from Rashba effect, but did not address the nature of Kondo pairing itself.

J. H. H. is supported by NRF grant (No. 2010-0008529, 2011-0015631) and acknowledges discussion with Yuji Matsuda that inspired this project.

---

\* Electronic address: [phyruth@gmail.com](mailto:phyruth@gmail.com)

- [1] H. Shishido, T. Shibauchi, K. Yasu, T. Kato, H. Kontani, T. Terashima, and Y. Matsuda, *Science* **327**, 980 (2010).
- [2] Y. Mizukami, H. Shishido, T. Shibauchi, M. Shimozawa, S. Yasumoto, D. Watanabe, M. Yamashita, H. Ikeda, T. Terashima, H. Kontani, and Y. Matsuda, *Nat. Phys.* **7**, 849 (2011).
- [3] E. Bauer, G. Hilscher, H. Michor, C. Paul, E. W. Scheidt, A. Griбанov, Y. Seropegin, H. Noël, M. Sigrist, and P. Rogl, *Phys. Rev. Lett.* **92** 027003 (2004).
- [4] Daisuke Maruyama, Manfred Sigrist, and Youichi Yanase, *J. Phys. Soc. Jpn.* **81**, 034702 (2012).
- [5] L. Petersen and P. Hedegård, *Surf. Sci.* **459**, 49 (2000).
- [6] Seung Ryong Park, Choong H. Kim, Jaejun Yu, Jung Hoon Han, and Changyoung Kim, *Phys. Rev. Lett.* **107**, 156803 (2011).
- [7] Jin-Hong Park, Choong H. Kim, Jun-Won Rhim, and Jung Hoon Han, *Phys. Rev. B* **85**, 195401 (2012).
- [8] Takahiro Maehira, Takashi Hotta, Kazuo Ueda, and Akira Hasegawa, *J. Phys. Soc. Jpn.* **72**, 854 (2003).
- [9] D. L. Cox, *Exotic Kondo Effects in Metals: Magnetic Ions in a Crystalline Electric Field and Tunnelling Centres* (Taylor & Francis, London, 1999).
- [10] Pouyan Ghaemi and T. Senthil, *Phys. Rev. B* **75**, 144412 (2007).
- [11] Heidrun Weber and Matthias Vojta, *Phys. Rev. B* **77**, 125118 (2008).
- [12] Pouyan Ghaemi, T. Senthil, and P. Coleman, *Phys. Rev. B* **77**, 245108 (2008).
- [13] One can show that this statement is consistent with Table I after allowing for the double degeneracy of the state due to vanishing  $\gamma$  and the U(1) gauge freedom of eigenvectors.
- [14] Jin-Hong Park, Choong H. Kim, Hyun-Woo Lee, and Jung Hoon Han, *Phys. Rev. B* **87**, 041301(R) (2013).